Nuclear Instruments and Methods in Physics Research B 554 (2024) 165415

Contents lists available at ScienceDirect

Nuclear Inst. and Methods in Physics Research, B

journal homepage: www.elsevier.com/locate/nimb

Charge state distributions of Xenon ions with keV kinetic energies transmitted through graphene and carbon self-supporting foils

R. Holeňák *, E. Ntemou, D. Primetzhofer

Department of Physics and Astronomy, Uppsala University, Box 516, 751 20 Uppsala, Sweden

ARTICLE INFO

Keywords:
Ion transmission
Equilibrium charge state
Xenon
Charge-exchange
Graphene

ABSTRACT

We investigated the charge state distributions and energy loss of single and double-charged Xenon ions (20–220 keV) passing through graphene, Quantifoil, and 10 nm thick carbon membranes. Utilizing simultaneous carbon recoil detection on the graphene-containing sample, we determined the areal density of carbon equivalent to 3 monolayers of graphene, indicating only slight contamination by e.g. PMMA, of our exiting surfaces. The charge state distributions revealed notable proportions of higher charge states, up to Xe^{+5} at higher energies, with mean charge states consistently below 1. The observed exponential decrease in higher charge fractions suggests electron stripping processes play a significant role. Differences in mean charge states are found among the three systems studied.

1. Introduction

Heavy highly charged ions (HCIs) offer a promising avenue for large-scale near-surface modifications encompassing a diverse range of applications, from nano-structuring of thin films to the fabrication of pores in self-supporting membranes or selective sputtering of 2D materials stacks such as graphene and MoS_2 [1–6]. The decisive aspect of these approaches lies in the controlled localization of energy deposition by HCIs. The high charge of the projectile interacts with the target via two pathways: firstly, by deposition of its high potential energy before entering the solid and consequently by increased preequilibrium kinetic energy loss [7,8]. While slow HCIs exhibit charge states that by far exceed the mean equilibrium charge states expected at their respective kinetic energy within solids [9], fast HCIs can be tuned to initially carry both higher or lower charges than the expected equilibrium charge state [10]. Inside a solid, projectiles with charge states above equilibrium bring up the concept of an incomplete screening, which persists for a few femtoseconds, contributing to enhancements in electronic excitations [11,12]. Accurate knowledge of charge equilibration times can significantly enhance our comprehension of nanoscale energy transfer mechanisms in the preequilibrium regime. Several groups have worked on a comprehensive understanding of the deexcitation mechanisms [13] using slow highly charged ions like Xenon transmitted through single and multilayers of 2D materials [14,15].

Due to the complex nature of the interaction between projectile and target a calculation of the equilibrium charge from first principles is highly complex [16]. For very slow noble gas projectiles $v/v_0 \ll 1$, the final charge state is expected to be zero or near-zero, since, depending on the electronic structure of the projectile Auger or resonant neutralization dominates over electron loss processes [17]. Several studies have suggested that heavy elements at keV energies have the potential to undergo close collision-induced inner-shell ionization due to the formation of molecular orbitals resulting in large energy losses and a formation of projectiles with higher charge fractions [18–20]. Nevertheless, in a highly asymmetric system like Xe-C and at energies below 1.7 keV/amu these excitation channels are not expected to be active [21,22]. The charge exchange dynamic is rather expected to resemble what is observed in low-energy ion scattering [17]. In the absence of an efficient predictive modelling of charge state formation in solid, experimental charge state distribution data provides empirical information on the underlying physics e.g. equilibrium stopping power, how much is it exceeded and also how fast the equilibrium is reached. While the literature on equilibrium charge state distributions of low-Z projectiles in carbon is extensive [23–26], investigations involving Xenon projectiles at energies below 300 keV are absent, despite their broad usage in fundamental investigations.

In this contribution, we provide charge distributions of keV Xenon ions transmitted through different carbon-based membranes. Utilizing a time-of-flight approach, we simultaneously detect all charge fractions, including neutral particles. Three systems including as-purchased

* Corresponding author.
E-mail address: radek.holenak@physics.uu.se (R. Holeňák).

https://doi.org/10.1016/j.nimb.2024.165415
Received 8 January 2024; Received in revised form 16 May 2024; Accepted 31 May 2024
Available online 7 June 2024

graphene, Quantifoil and a 10 nm thick carbon membrane were used as targets. A recently introduced medium energy time-of-flight based elastic recoil detection technique [27] is applied to accurately determine the effective thickness of the contaminated graphene sample. High charge fractions up to +5 were detected at the highest energies. Differences observed in the obtained charge states among different foils are briefly discussed.

2. Method

Experiments were performed with the time-of-flight medium energy ion scattering (ToF-MEIS) setup at Uppsala University [28,29]. A chopped beam of single or doubly charged atomic ions is delivered on the sample within a beam spot usually smaller than 1x1 mm^2 and beam angular divergence ~ 0.056°. The short pulses of the beam ensure that the current impinging on the membranes is below pA and induces virtually no damage. The effective ion number per pulse is found significantly below 1 guaranteeing the absence of potential coincidence losses. The rotatable position-sensitive multichannel plate detector was positioned in transmission geometry 290 mm down the beam axis from the metal openings featuring the thin foil targets. As targets we employed as-purchased single-layer graphene (SLG) from Graphenea [30] prepared as a stack of copper TEM grid/Quantifoil [31]/graphene mounted with the graphene layer facing the incoming beam. As no surface treatment was performed, considerable contamination by PMMA is expected on the graphene surface as a consequence of the transfer process with up to a few nm thick polymer layers reported earlier [32–34]. Along with the graphene, we also evaluated the charge distributions of projectiles transmitted through the supporting Quantifoil membrane with an expected thickness of 15–20 nm. Though the bulk material of Quantifoil is carbon, the fabrication process is facilitated by the use of a photoresist and other organic chemicals, presumed to remain on the surface [31]. As a third system, we used a 10 nm thick self-supporting carbon foil fabricated by carbon deposition on a microscopic glass covered with a water-soluble layer. The purchased foils were floated in the water bath and extended over a metal frame [26].

An example of the recorded ToF spectrum for 20 keV $^{129}Xe^{+}$ is displayed in Fig. 1. The two dominant peaks around a flight time of 1686 ns belong to the unperturbed beam passing through pinholes and damaged area in the target (accounting for less than 4 % in the irradiated area) and to projectiles transmitted through the graphene sample. The thickness of the supporting Quantifoil did not permit any Xenon projectile to exit the membrane at the given energy. Due to the known sample-detector distance, the time delay between the ToF peaks can be converted to the mean energy loss. The target recoils observed at shorter flight times with low intensity originate from near head-on collisions with the impinging Xenon projectiles. The two peaks assigned to hydrogen and carbon recoils were fitted by two overlapping skewed gaussian. The integrated area under the carbon recoil peak was subsequently converted into an effective thickness of the membrane [27]. Using the collected Xenon projectiles as a total number of impinging ions and by applying differential recoil cross-section with ZBL screening [35], the calculated thickness of the carbon layer was determined to be equivalent to ~ 3 times the surface density of graphene. A considerably large error emerges from the overlap between hydrogen and carbon recoil peaks and the ambiguity in the applicable background subtraction and peak integration. Moreover, the recorded low energy losses of 500 eV for 20 keV ^{129}Xe and 570 eV for 40 keV ^{132}Xe further corroborate that the transmission occurred through a sub-nanometer thin layer. The energy losses were not extracted for any of the faster projectiles due to the limited energy resolution of about 1 keV at higher velocities.

Detection of the charge fraction of the transmitted beam was enabled by employing a deflection apparatus as introduced in [26] consisting of a narrow vertical slit and electrostatically charged metal plates. After transmission through the target, projectiles with different charges are separated within the deflection unit parallel to the beam axis and arrive on the detection plate in the form of vertical bands (see Fig. 1b). The counts within a small rectangular area in the centre of each band corresponding to a deflection of less than 0.2 degrees are separately integrated. The derived charge fractions are then normalized to the sum of all integrated counts. The error bars consider only statistical uncertainties; however, a further scattering of the data points might occur due to an imperfect alignment between the beam and deflector. Due to the almost negligible energy loss of the projectiles in the graphene samples, their charge distributions are presented as a function of the initial energy. For the carbon and Quantifoil samples, the detected energy was used.

3. Results and discussion

Fig. 2a and 2b show charge state distributions recorded for Xenon projectiles transmitted through graphene and carbon membrane in linear and logarithmic scales, respectively. Throughout the covered energy range, 90 % of the detected projectiles are either neutrals or singly positively charged. In the remaining 10 %, charges up to +5 are represented. At given energy, the incrementally higher charge fractions are decreasing by an order of magnitude in their abundance. Such exponential behaviour is characteristic to a statistical process governed

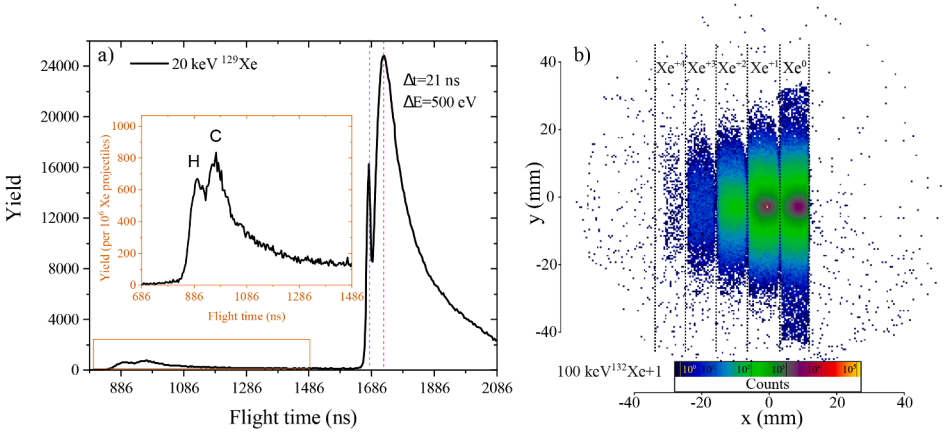

Fig. 1. A) time-of-flight spectrum recorded with 20 keV ^{129}Xe impinging on the graphene sample featuring two dominant peaks associated with transmitted Xenon projectiles through holes and graphene, respectively. Recoils of hydrogen and carbon used for thickness determination are magnified in the inset. b) 2D distribution of 100 keV ^{132}Xe projectiles in the detection plane after passage through the deflection apparatus. The band corresponding to Xe^{0} (zero deflection) is positioned around x = 7 mm. The bright spot in the middle of the +1 band belongs to the steered unperturbed Xe^{+1} beam passing through holes.

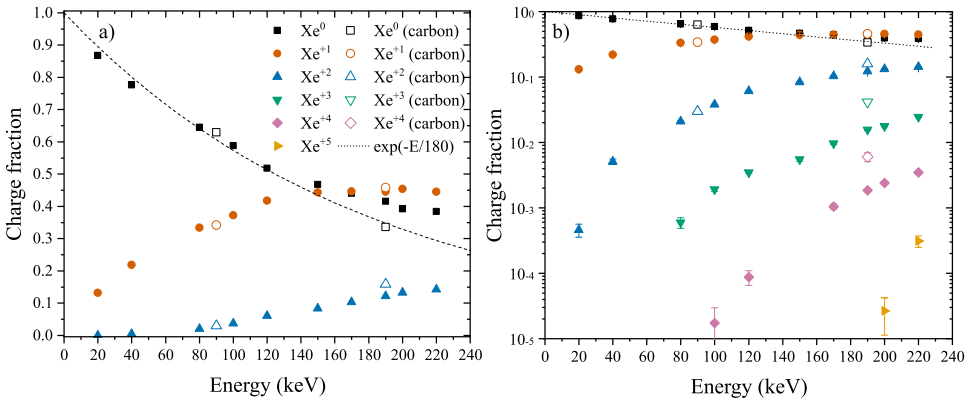

Fig. 2. Charge state fractions of Xenon after transmission through contaminated graphene and 10 nm thick carbon foil plotted as a function of energy in a) linear and b) logarithmic scale. An exponential fit was performed on the neutral fractions recorded for graphene up to 120 keV.

by rate equations e.g. electron stripping phenomena [36]. At low energies, data for graphene and carbon are in good agreement. However, a discrepancy in the respective fractions is found at higher energies. By introducing an exponential fit to the data points of the neutral fraction of graphene for energies up to 120 keV, we observed that the neutral fractions from the carbon membrane follow the expected exponential trend throughout the energy range, while data for graphene shows a change in slope in the direction of an increased amount of neutrals at the expense of the presence of higher charge fractions. No change in distribution is observed when using Xenon projectiles with the charge +2 applied in measuring graphene data points at 190 keV and 220 keV, indicating that the transit times are long enough to equilibrate the incoming projectiles before exiting the foil.

A single representative value can be ascribed to the charge distribution at a given energy by defining its mean. A compilation of all acquired data can thus be plotted in a single graph (Fig. 3), this time presented as a function of ion velocity. Along with our experiments, equilibrium mean charges derived from the work of Loew [37] and mean charge state measured using highly charged Xenon [11] for higher energies are shown. The experimental data are complemented by a theoretical curve of Bohr [36] and a semiempirical curve from the work of Schiwietz and Grande [38], acknowledging their limited validity for low

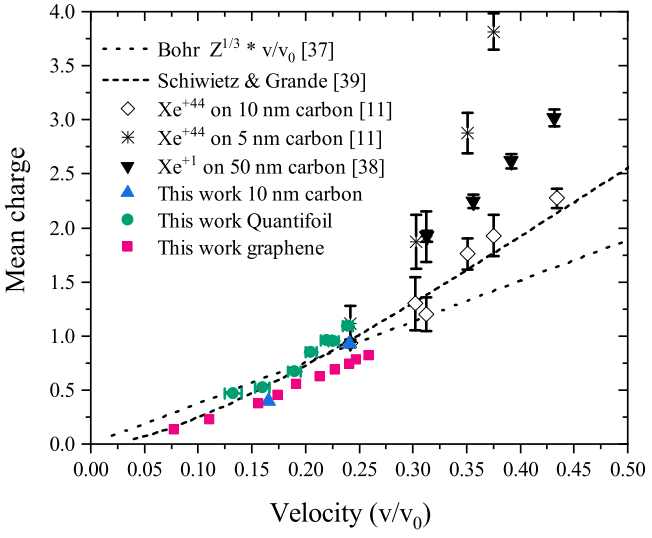

Fig. 3. Mean of the charge distributions of Xenon after transmission through a number of carbon-based foils plotted as a function of Bohr's velocity. Literature data on mean equilibrium and preequilibrium mean charges of Xenon at higher energies were taken from Loew [37] and Hattass et al. [11], respectively. Predictions by Bohr [36] and Schiwietz et. al. [38] are provided.

velocities. The first observation is that our experimental data for the Quantifoil show consistently higher mean charge compared to data from graphene and carbon. A discrepancy is furthermore observed in the literature, where both datasets collected using HCIs were expected to remain in their preequilibrated state, however, the mean equilibrium charge measured by Loew lies in-between the two datasets. Where our data overlap with the literature, excellent agreement is found between mean charges measured on carbon membranes with the same thickness of 10 nm. However, the discrepancy among all measurements at the given velocity of 0.25 v_0 is around 20 %. Within these margins, both theoretical predictions succeed to provide a reasonable estimate of the average equilibrium value.

Though referred to as an equilibrium charge, the experimentally acquired charge fractions are known to be heavily influenced by the surface of the target [39,40]. Few monolayers of foreign atoms can easily alter the final charge distributions towards either side [41,42]. For the most reliable charge measurements, it is therefore necessary to ensure atomically clean surfaces [43]. Even though the most common surface contamination are carbon-based molecules, the chemical bonds the carbon atoms reside in can still have an effect on the charge transfer between the target and projectile [44,45]. The differences observed in our experiment indicate that the three predominately carbon-containing systems do not interact with the projectile in an identical manner. Considering the equilibration timescales of highly charged Xenon projectiles in carbon and graphene collectively reported on in [10], the equilibrium charge state for the fastest projectile used in our experiments should be reached within the first 1 nm. Inside the solid, the projectile interaction with surrounding electrons leads predominately to the target excitation and a graduate energy loss of the projectile. The equilibrium charge inside the solid is established when the electron capture and electron loss rates are in equilibrium. The true nature of the charge-exchange processes is, however, not trivial since the specific electronic structure and thus the momentum distribution of valence and conduction electrons of the target material are expected to become relevant at these low energies [46]. Similar to low-energy ion scattering, one can assume, that while neutralization by non-local Auger processes may show only a weak dependence on interaction distance, ionization processes will exhibit a different dependence [47]. At the exit surface, Auger neutralization will dominate over electron loss and is expected to shift the observed charge distribution towards lower values in comparison to the values in the solid.

In this notion, the observed discrepancies in the mean charge among the studied system can have origin in both the differences in the ionization probabilities inside the targets as well as in a change in neutralization dynamics on the exit surfaces. Previous work in low-energy helium ion scattering conducted on carbon-based materials including graphene exemplified the influence of carbon hybridization on the neutralization effectiveness [45]. Silicone rubber with sp^3 hybridization

was shown to preserve a higher fraction of the charged projectiles compared to the sp^2 hybridized graphitic sample. In our systems, both carbon foil and graphene have sp^2 hybridization, while the Quantifoil and surface contaminants like PMMA and alcohol feature likely a combination of both sp^2 and sp^3 hybridizations. This phenomenon presents a plausible explanation for the scaling of the observed differences, with the graphene-containing sample showing the lowest fraction of the charged projectiles and Quantifoil the highest. Moreover, our data at lower velocities showing equivalent charge state after transmission through 10 nm of carbon and the ultrathin graphene membrane indicate extremely effective charge transfer by graphene in alignment with the interpretation above and earlier observations for highly charged ions [48].

4. Summary

We have provided charge state distributions of Xenon projectiles transmitted through a commercially purchased single layer of graphene, a Quantifoil and a 10 nm carbon foil. Utilizing the time-of-flight technique we were not only able to detect all charge states simultaneously but by evaluating the recoil yields also determined the average thickness of the contaminated graphene sample equivalent to approximately 3 monolayers of graphene. Higher charge fractions reaching up to Xe^{+5} were found at all energies and should be considered when exploring the deexcitation dynamics and equilibrium stopping power of HCIs. The differences in composition and structure, as well as surface properties among the studied systems, can play an important role affecting in particular neutralization probabilities similar to what has been observed in low-energy scattering.

Declaration of competing interest

The authors declare that they have no known competing financial interests or personal relationships that could have appeared to influence the work reported in this paper.

Acknowledgements

Accelerator operation is supported by the Swedish Research Council VR-RFI (Contract No. 2019-00191).

References

[1] R. Ritter, R.A. Wilhelm, M. Stöger-Pollach, R. Heller, A. Mücklich, U. Werner, H. Vieker, A. Beyer, S. Facsko, A. Gölzhäuser, F. Aumayr, Fabrication of nanopores in 1 nm thick carbon nanomembranes with slow highly charged ions, Appl. Phys. Lett. 102 (2013) 063112, https://doi.org/10.1063/1.4792511.

[2] T. Schenkel, M.A. Briere, H. Schmidt-Böcking, K. Bethge, D.H. Schneider, Electronic sputtering of thin conductors by neutralization of slow highly charged ions, Phys. Rev. Lett. 78 (1997) 2481–2484, https://doi.org/10.1103/PhysRevLett.78.2481.

[3] R. Heller, S. Facsko, R.A. Wilhelm, W. Möller, Defect mediated desorption of the KBr(001) surface induced by single highly charged ion impact, Phys. Rev. Lett. 101 (2008) 096102, https://doi.org/10.1103/PhysRevLett.101.096102.

[4] A.S. El-Said, R.A. Wilhelm, R. Heller, M. Sorokin, S. Facsko, F. Aumayr, Tuning the fabrication of nanostructures by low-energy highly charged ions, Phys. Rev. Lett. 117 (2016) 126101, https://doi.org/10.1103/PhysRevLett.117.126101.

[5] L. Madauß, I. Zegkinoglou, H. Vázquez Muiños, Y.W. Choi, S. Kunze, M.Q. Zhao, C. H. Naylor, P. Ernst, E. Pollmann, O. Ochedowski, H. Lebius, A. Benyagoub, B. Band'Etat, A.T.C. Johnson, F. Djurabekova, B. Roldan Cuenya, M. Schleberger, Highly active single-layer MoS 2 catalysts synthesized by swift heavy ion irradiation, Nanoscale 10 (2018) 22908–22916, https://doi.org/10.1039/C8NR04696D.

[6] R.S. Thomaz, P. Ernst, P.L. Grande, M. Schleberger, R.M. Papaléo, Cratering induced by slow highly charged ions on ultrathin PMMA films, Atoms. 10 (2022) 96, https://doi.org/10.3390/atoms10040096.

[7] T. Schenkel, M.A. Briere, A.V. Barnes, A.V. Hamza, K. Bethge, H. Schmidt-Böcking, D.H. Schneider, Charge state dependent energy loss of slow heavy ions in solids, Phys. Rev. Lett. 79 (1997) 2030–2033, https://doi.org/10.1103/PhysRevLett.79.2030.

[8] R.A. Wilhelm, E. Gruber, V. Smejkal, S. Facsko, F. Aumayr, Charge-state-dependent energy loss of slow ions. I. Experimental results on the transmission of highly charged ions, Phys. Rev. a. 93 (2016) 052708, https://doi.org/10.1103/PhysRevA.93.052708.

[9] S. Creutzburg, A. Niggas, D. Weichselbaum, P.L. Grande, F. Aumayr, R.A. Wilhelm, Angle-dependent charge exchange and energy loss of slow highly charged ions in freestanding graphene, Phys. Rev. a. 104 (2021) 042806, https://doi.org/10.1103/PhysRevA.104.042806.

[10] P. Ström, D. Primetzhofer, Energy deposition by nonequilibrium charge states of MeV i 127 in Au, Phys. Rev. a. 103 (2021) 022803, https://doi.org/10.1103/PhysRevA.103.022803.

[11] M. Hattass, T. Schenkel, A.V. Hamza, A.V. Barnes, M.W. Newman, J.W. McDonald, T.R. Niedermayr, G.A. Machicoane, D.H. Schneider, Charge equilibration time of slow, highly charged ions in solids, Phys. Rev. Lett. 82 (1999) 4795–4798, https://doi.org/10.1103/PhysRevLett.82.4795.

[12] J.I. Juaristi, A. Arnau, P.M. Echenique, C. Auth, H. Winter, Charge state dependence of the energy loss of slow ions in metals, Phys. Rev. Lett. 82 (1999) 1048–1051, https://doi.org/10.1103/PhysRevLett.82.1048.

[13] T. Jahnke, Interatomic and intermolecular Coulombic decay: The coming of age story, J. Phys. B at. Mol. Opt. Phys. 48 (2015) 082001, https://doi.org/10.1088/0953-4075/48/8/082001.

[14] R.A. Wilhelm, P.L. Grande, Unraveling energy loss processes of low energy heavy ions in 2D materials, Commun. Phys. 2 (2019) 89, https://doi.org/10.1038/s42005-019-0188-7.

[15] A. Niggas, J. Schwestka, K. Balzer, D. Weichselbaum, N. Schlünzen, R. Heller, S. Creutzburg, H. Inani, M. Tripathi, C. Speckmann, N. McEvoy, T. Susi, J. Kotakoski, Z. Gan, A. George, A. Turchanin, M. Bonitz, F. Aumayr, R.A. Wilhelm, Ion-induced surface charge dynamics in freestanding monolayers of graphene and MoS2 probed by the emission of electrons, Phys. Rev. Lett. 129 (2022) 086802, https://doi.org/10.1103/PhysRevLett.129.086802.

[16] K. Balzer, M. Bonitz, Neutralization dynamics of slow highly charged ions passing through graphene nanoflakes: An embedding self-energy approach, Contrib. to Plasma Phys. 62 (2022) e202100041.

[17] H. Brongersma, M. Draxler, M. de Ridder, P. Bauer, Surface composition analysis by low-energy ion scattering, Surf. Sci. Rep. 62 (2007) 63–109, https://doi.org/10.1016/j.surfrep.2006.12.002.

[18] M.J. Gordon, J. Mace, K.P. Giapis, Charge-exchange mechanisms at the threshold for inelasticity in Ne+ collisions with surfaces, Phys. Rev. a. 72 (2005) 012904, https://doi.org/10.1103/PhysRevA.72.012904.

[19] A.N. Zinoviev, P.Y. Babenko, A.P. Shergin, Formation and decay of autoionization states as the main inelastic energy loss mechanism in keV atomic collisions, J. Exp. Theor. Phys. 136 (2023) 662–681, https://doi.org/10.1134/S1063776123050138.

[20] S. Lohmann, R. Holeňák, D. Primetzhofer, Trajectory-dependent electronic excitations by light and heavy ions around and below the Bohr velocity, Phys. Rev. a. 102 (2020) 062803, https://doi.org/10.1103/PhysRevA.102.062803.

[21] D.H.G. Schneider, M.A. Briere, Investigations of the interactions of highest charge state ions with surfaces, Phys. Scr. 53 (1996) 228–242, https://doi.org/10.1088/0031-8949/53/2/013.

[22] R. Schuch, D. Schneider, D.A. Knapp, D. DeWitt, J. McDonald, M.H. Chen, M. W. Clark, R.E. Marrs, Evidence for internal dielectronic excitation of slow highly charged uranium ions, Phys. Rev. Lett. 70 (1993) 1073–1076, https://doi.org/10.1103/PhysRevLett.70.1073.

[23] K. Shima, N. Kuno, M. Yamanouchi, H. Tawara, Equilibrium charge fractions of ions of Z = 4–92 emerging from a carbon foil, At. Data Nucl. Data Tables. 51 (1992) 173–241, https://doi.org/10.1016/0092-640X(92)90001-X.

[24] P.L. Grande, G. Schiwietz, Improved calculations of the electronic energy loss under channeling conditions, Nucl. Instruments Methods Phys. Res. Sect. B Beam Interact. with Mater. Atoms. 136–138 (1998) 125–131, https://doi.org/10.1016/S0168-583X(97)00869-0.

[25] A. Bürgi, M. Oetliker, P. Bochsler, J. Geiss, M.A. Coplan, Charge exchange of low-energy ions in thin carbon foils, J. Appl. Phys. 68 (1990) 2547–2554, https://doi.org/10.1063/1.346478.

[26] R. Holeňák, S. Lohmann, F. Sekula, D. Primetzhofer, Simultaneous assessment of energy, charge state and angular distribution for medium energy ions interacting with ultra-thin self-supporting targets: A time-of-flight approach, Vacuum 185 (2021) 109988, https://doi.org/10.1016/j.vacuum.2020.109988.

[27] R. Holeňák, S. Lohmann, D. Primetzhofer, Sensitive multi-element profiling with high depth resolution enabled by time-of-flight recoil detection in transmission using pulsed keV ion beams, Vacuum 204 (2022) 111343, https://doi.org/10.1016/j.vacuum.2022.111343.

[28] M.K. Linnarsson, A. Hallén, J. Åström, D. Primetzhofer, S. Legendre, G. Possnert, New beam line for time-of-flight medium energy ion scattering with large area position sensitive detector, Rev. Sci. Instrum. 83 (2012) 095107, https://doi.org/10.1063/1.4750195.

[29] M.A. Sortica, M.K. Linnarsson, D. Wessman, S. Lohmann, D. Primetzhofer, A versatile time-of-flight medium-energy ion scattering setup using multiple delay-line detectors, Nucl. Instruments Methods Phys. Res. Sect. B Beam Interact. with Mater. Atoms. 463 (2020) 16–20, https://doi.org/10.1016/j.nimb.2019.11.019.

[30] Graphenea, (2024). https://www.graphenea.com/.

[31] E. Ermantraut, K. Wohlfart, W. Tichelaar, Perforated support foils with pre-defined hole size, shape and arrangement, Ultramicroscopy 74 (1998) 75–81, https://doi.org/10.1016/S0304-3991(98)00025-4.

[32] Y.C. Lin, C. Jin, J.C. Lee, S.F. Jen, K. Suenaga, P.W. Chiu, Clean transfer of graphene for isolation and suspension, ACS Nano 5 (2011) 2362–2368, https://doi.org/10.1021/nn200105j.

[33] M. Kratzer, B.C. Bayer, P.R. Kidambi, A. Matković, R. Gajić, A. Cabrero-Vilatela, R. S. Weatherup, S. Hofmann, C. Teichert, Effects of polymethylmethacrylate-transfer residues on the growth of organic semiconductor molecules on chemical vapor deposited graphene, Appl. Phys. Lett. 106 (2015) 103101, https://doi.org/10.1063/1.4913948.

[34] X. Li, Y. Zhu, W. Cai, M. Borysiak, B. Han, D. Chen, R.D. Piner, L. Colomba, R. S. Ruoff, Transfer of large-area graphene films for high-performance transparent conductive electrodes, Nano Lett. 9 (2009) 4359–4363, https://doi.org/10.1021/nl902623y.
[35] J.F. Ziegler, J.P. Biersack, The Stopping and Range of Ions in Matter, in: D.A. Bromley (Ed.), Treatise Heavy-Ion Sci. Vol. 6 Astrophys. Chem. Condens. Matter, Springer US, Boston, MA, 1985: pp. 93–129. https://doi.org/10.1007/978-1-4615-8103-1_3.
[36] N. Bohr, The penetration of atomin particles through matter, Dan. Videns. Sels. Mat-Fys. Medd. 28 (1948).
[37] R. Loew, Charge-state and energy distributions of Xenon ions in carbon, Nucl. Instruments Methods. 118 (1974) 505–508, https://doi.org/10.1016/0029-554X(74)90658-2.
[38] G. Schiwietz, P. Grande, Improved charge-state formulas, Nucl. Instruments Methods Phys. Res. Sect. B Beam Interact. with Mater. Atoms. 175–177 (2001) 125–131, https://doi.org/10.1016/S0168-583X(00)00583-8.
[39] J.A. Phillips, Charge equilibrium ratios for hydrogen ions from solids, Phys. Rev. 97 (1955) 404–410, https://doi.org/10.1103/PhysRev.97.404.
[40] T.M. Buck, G.H. Wheatley, L.C. Feldman, Charge states of 25–150 keV H and 4He backscattered from solid surfaces, Surf. Sci. 35 (1973) 345–361, https://doi.org/10.1016/0039-6028(73)90224-0.
[41] S. Kreussler, R. Sizmann, Neutralization of 50–230 keV hydrogen ions which have penetrated Al, Au, C, and Cs films, Phys. Rev. b. 26 (1982) 520–529, https://doi.org/10.1103/PhysRevB.26.520.
[42] K.H. Berkner, I. Bornstein, R.V. Pyle, J.W. Stearns, Charge Fractions and Excited-Atom Populations of 8–100 keV Deuterium Beams Emerging from Solid Films of C, Mg, Nb, and Au, Phys. Rev. a. 6 (1972) 278–288, https://doi.org/10.1103/PhysRevA.6.278.
[43] A. Niggas, J. Schwestka, S. Creutzburg, T. Gupta, D. Eder, B.C. Bayer, F. Aumayr, R. A. Wilhelm, The role of contaminations in ion beam spectroscopy with freestanding 2D materials: A study on thermal treatment, J. Chem. Phys. 153 (2020) 014702, https://doi.org/10.1063/5.0011255.
[44] L.C.A. van den Oetelaar, S.N. Mikhailov, H.H. Brongersma, Mechanism of neutralization in low-energy He+ ion scattering from carbidic and graphitic carbon species on rhenium, Nucl. Instruments Methods Phys. Res. Sect. B Beam Interact. with Mater. Atoms. 85 (1994) 420–423, https://doi.org/10.1016/0168-583X(94)95856-4.
[45] S. Průša, P. Procházka, P. Bábor, T. Šikola, R. ter Veen, M. Fartmann, T. Grehl, P. Brüner, D. Roth, P. Bauer, H.H. Brongersma, Highly sensitive detection of surface and intercalated impurities in graphene by LEIS, Langmuir 31 (2015) 9628–9635, https://doi.org/10.1021/acs.langmuir.5b01935.
[46] A. Lim, W.M.C. Foulkes, A.P. Horsfield, D.R. Mason, A. Schleife, E.W. Draeger, A. A. Correa, Electron elevator: excitations across the band gap via a dynamical gap state, Phys. Rev. Lett. 116 (2016) 043201, https://doi.org/10.1103/PhysRevLett.116.043201.
[47] D. Primetzhofer, M. Spitz, E. Taglauer, P. Bauer, Resonant charge transfer in low-energy ion scattering: Information depth in the reionization regime, Surf. Sci. 605 (2011) 1913–1917, https://doi.org/10.1016/j.susc.2011.07.006.
[48] E. Gruber, R.A. Wilhelm, R. Pétuya, V. Smejkal, R. Kozubek, A. Hierzenberger, B. C. Bayer, I. Aldazabal, A.K. Kazansky, F. Libisch, A.V. Krasheninnikov, M. Schleberger, S. Facsko, A.G. Borisov, A. Arnau, F. Aumayr, Ultrafast electronic response of graphene to a strong and localized electric field, Nat. Commun. 7 (2016) 13948, https://doi.org/10.1038/ncomms13948.